TEXT TO SUPPLEMENTARY MATERIAL

Supplementary Figure S1. Alignment of the predicted amino acid sequences of HMGB1 and HMGB2 from different species. The similarity between zebrafish HMGB1 and HMGB2 is 74%. Zebrafish HMGB1 similarity is 86 % compared to mammalian HMGB1. Compared to chicken and Xenopus tropicalis HMGB1, the similarity is 79%.

Supplementary Figure S2. Schematic map of the zebrafish *Hmgb1* gene transcript and the strategy used to downregulate *Hmgb1* expression with morpholino antisense oligonucleotides. MO1 flanks the translation initiation site, and is expected to block protein translation. MO2 was designed against the the intron splicing site at the 3 ´ end of exon 3, and is expected to cause deletion of exon 3. MO3 was designed against the intron splicing site at the 5´ end of exon 4, and could cause insertion of intron 4. All MOs were able to downregulate HMGB1 protein expression in vivo (see Fig. 2). HMGB1 5 mis MO incorporates five mis-pairs along the length of the HMGB1 MO1 oligo.

Supplementary Figure S3. Dorsal view of HMGB1/AMIGO1 double-immunostaining at the diencephalic region of 28 hpf larval whole mounts. The staining of both proteins close to the diencephalic ventricle is absent in MO1 morphants. Co-injection of *Hmgb1* mRNA with MO1 rescues HMGB1 and AMIGO1 expression; however, the staining is more diffuse compared to normal control. Abbreviations: Di, Diencephalon; DiV, Diencephalic Ventricle; DT, Dorsal Thalamus; Pr, Pretectum; TeO, Tectum Opticum. Scale Bars, 150 µm for the top row of panels (HMGB1 MO1), 100 µm for the middle row (HMGB1 MO1 + mRNA), 60 µm for the bottom row of the panels (Uninjected).

Supplementary Figure S4. Dorsal view of HMGB1/AMIGO1 double-immunostaining at the telencephalic region of 28 hpf larval whole mounts. Abbreviations: Tel, Telencephalon; Ve, Brain Ventricle; VT, Ventral Thalamus. Scale bar, 100 µm.

Supplementary Figure S5. High resolution view of HMGB1/AMIGO1 ectodomain double-immunostaining in diencephalic cells of 28 hpf larval whole mounts. Patchy detection is seen for both proteins that partially colocalize at the plasma membrane. HMGB1 displays a more diffuse staining compared to AMIGO1. Scale bar, 10 µm.

Supplementary Figure S6. HMGB1/AMIGO1 ectodomain immunostaining in 28 hpf larval posterior trunk. (A) Dorsal view. (B) Lateral view. Both proteins are detected in the notochord in a patchy pattern. Abbreviations: N, Notochord; Sp, Spinal cord; Mt, Myotome. Scale bar, 100 µm.

Supplementary Figure S7. Phenotypic changes in 30 hpf larvae due to downregulation of HMGB1 expression (the phenotype at a later stage, 5 dpf, is shown in Fig. 4). (A) Side view of the uninjected and MO1 injected larvae. The regions corresponding to diencephalon and telencephalon are morphologically perturbed and smaller in size compared to those in the wild-type control. The boundary of the diencephalic ventricle is obscure and the optic cup is reduced in size. (B) Rostral view of the larvae. The distance between the eyes and the forebrain size are reduced in the morphants. Abbreviations: CeP, Cerebellar Plate; Di, Diencephalon; DiV, Diencephalon Ventricle; Fp, Floorplate; H, Hindbrain; Hv, Hindbrain ventricle; M, midbrain; MHB, Midbrain-Hindbrain Boundary; N, Notochord; Oc, Optical cup; Ot, Otic vesicle; Tel, Telencephalon; Scale bars, 200 µm in A, 100 µm in B.

Supplementary Figure S8. p53 MO coinjection effects. (A) Quantitative RT-PCR of p53 in 2dpf larval samples. Any of the HMGB1 MOs does not increase p53 expression but, in contrast, decreases it. (B) Quantitative RT-PCR of Δp53 (another isoform of p53 initiated from an internal promoter in intron 4 of the full-length transcript). Δp53 transcription is suppressed by the HMGB1 MOs in a similar manner as compared to p53 transcription. (C) Morphological phenotypes. HMGB1 MO1 injected larvae and HMGB1 MO1 plus p53 MO coinjected larvae display a very similar outlook with shorter head and curled tail. The p53 MO does not rescue morphological defects in the HMGB1 morphant.

Figure S1.

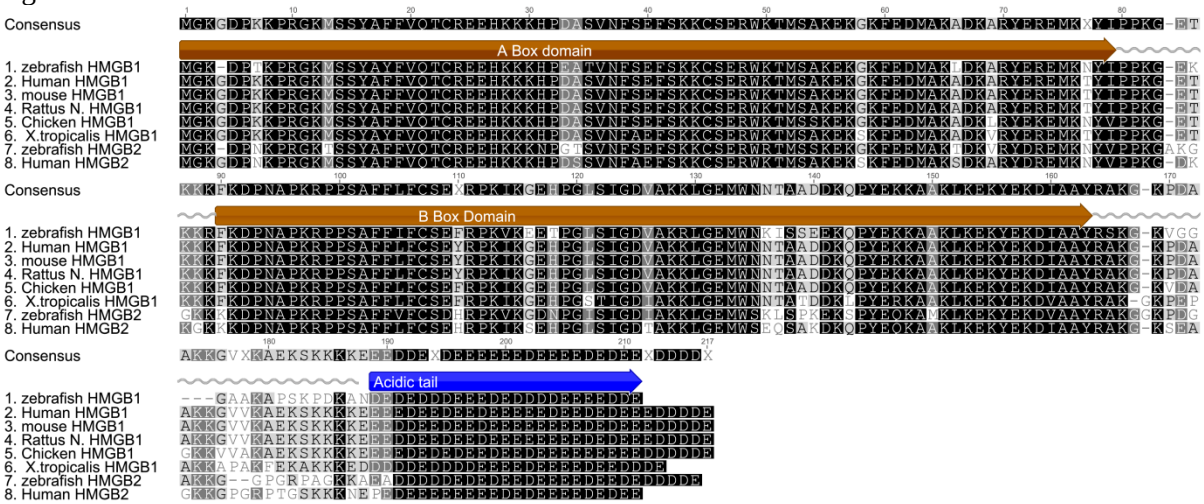

Figure S2.

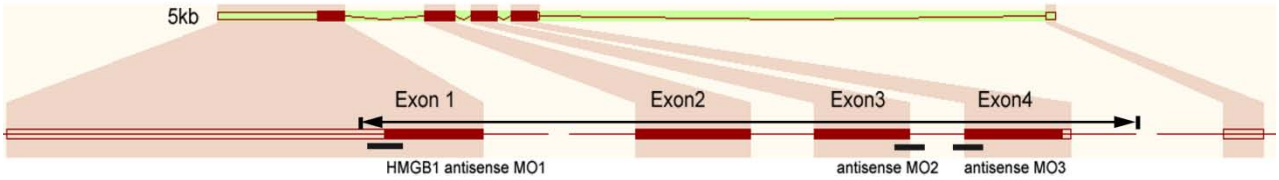

Figure S3.

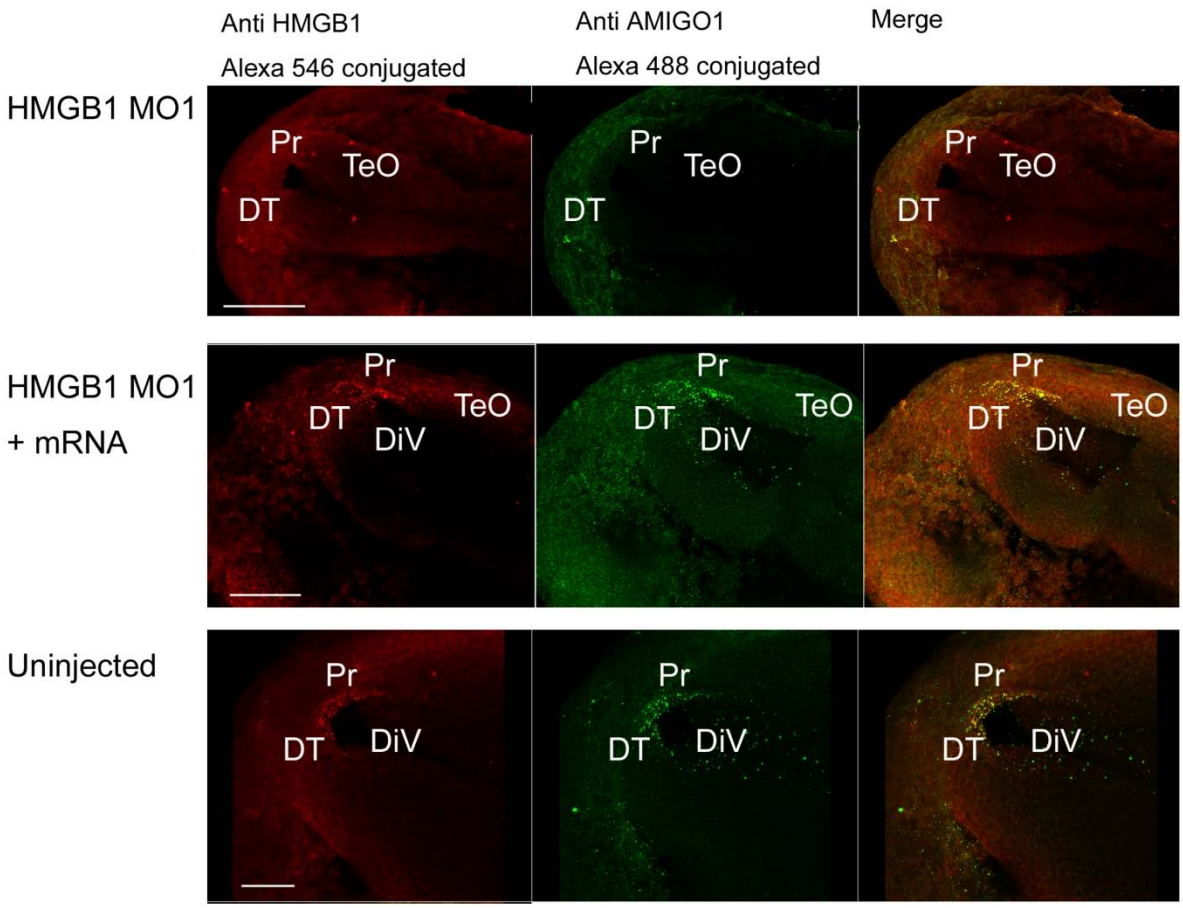
Anti HMGB1
Alexa 546 conjugated
Anti AMIGO1
Alexa 488 conjugated
Merge
HMGB1 MO1
HMGB1 MO1
+ mRNA
Uninjected
Pr
TeO
DT
DiV

Figure S4.

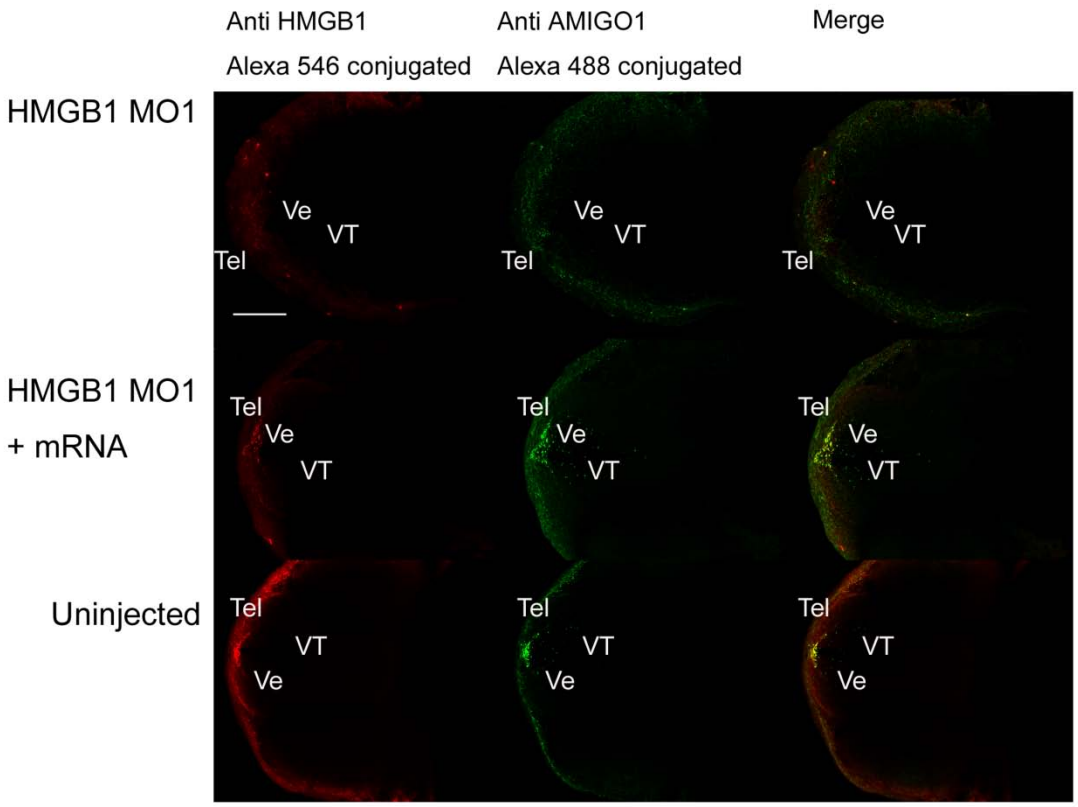
Anti HMGB1
Alexa 546 conjugated
Anti AMIGO1
Alexa 488 conjugated
Merge
HMGB1 MO1
HMGB1 MO1
+ mRNA
Uninjected
Tel
Ve
VT

Figure S5.

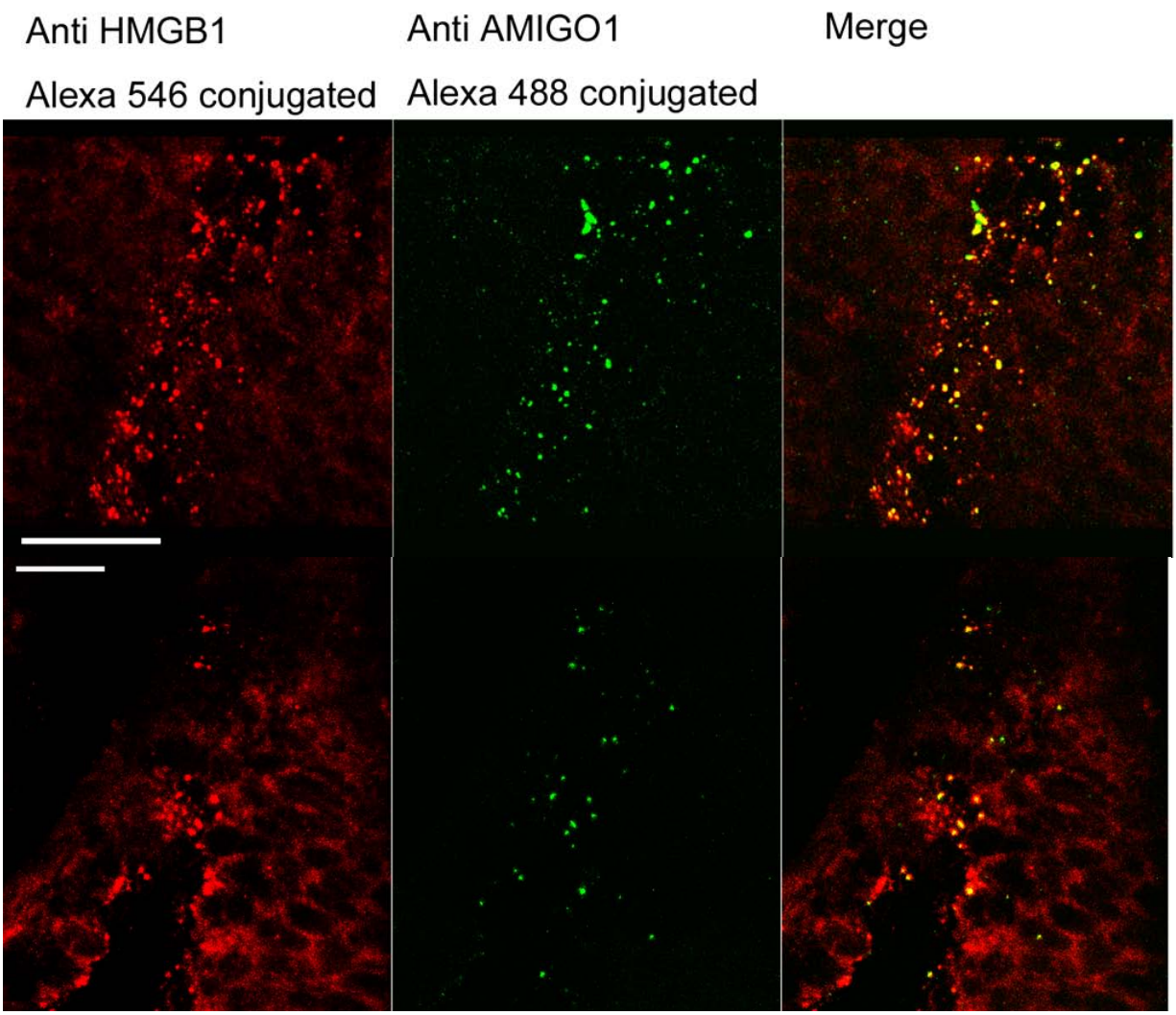
Anti HMGB1
Alexa 546 conjugated
Anti AMIGO1
Alexa 488 conjugated
Merge

Figure S6.

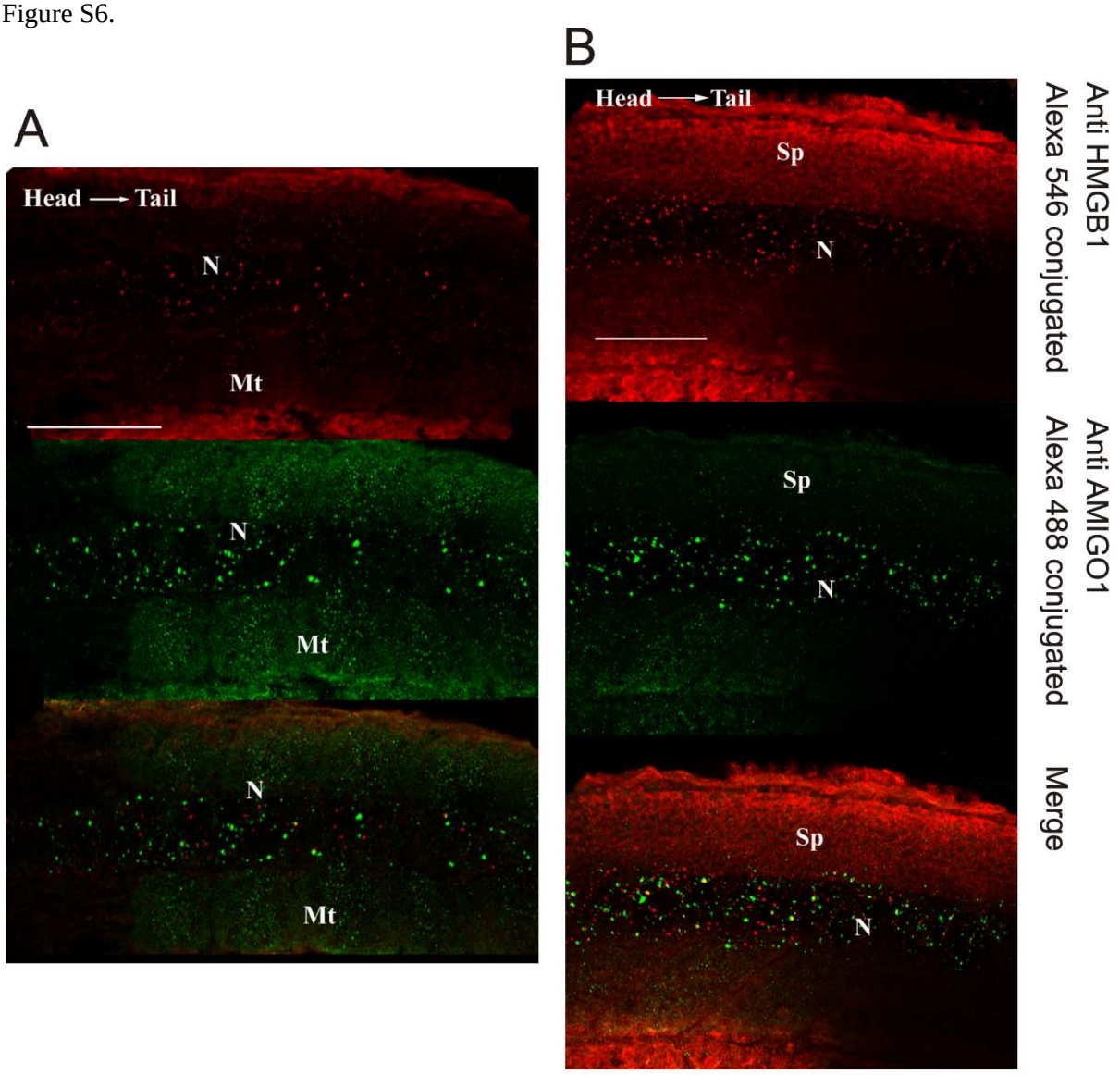
A
Head → Tail
N
Mt
N
Mt
N
Mt
B
Head → Tail
Sp
N
Sp
N
Sp
N
Anti HMGB1
Alexa 546 conjugated
Anti AMIGO1
Alexa 488 conjugated
Merge

Figure S7.

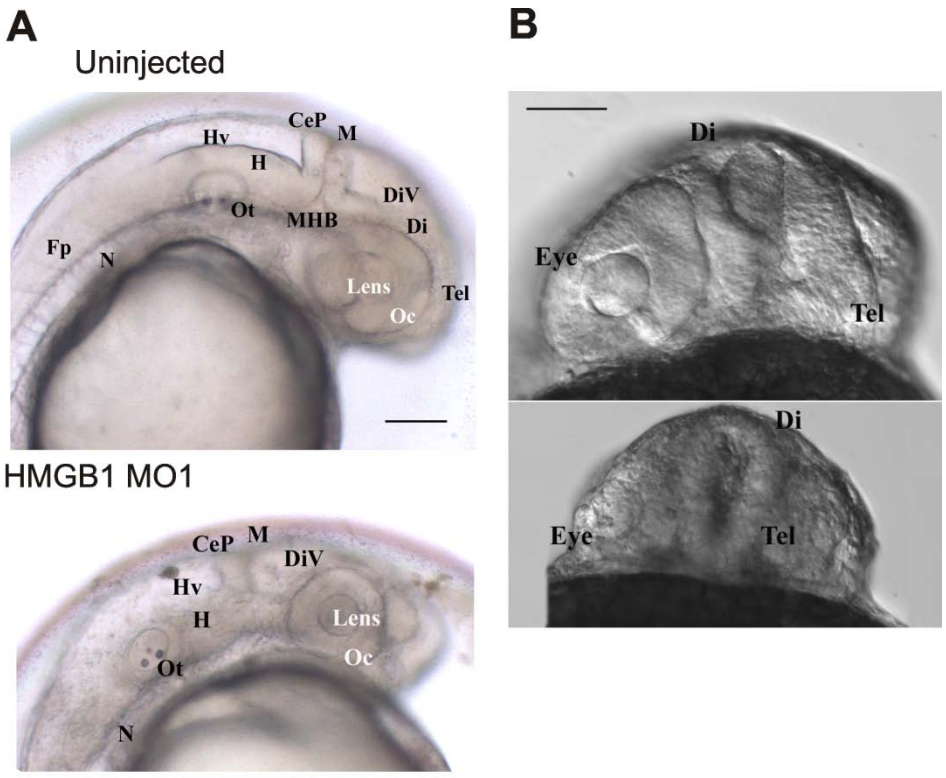
A
Uninjected
CeP
M
Hv
H
DiV
Ot
MHB
Di
Fp
N
Lens
Tel
Oc
HMGB1 MO1
CeP
M
DiV
Hv
H
Lens
Oc
Ot
N
B
Di
Eye
Tel
Di
Eye
Tel

Figure S8.

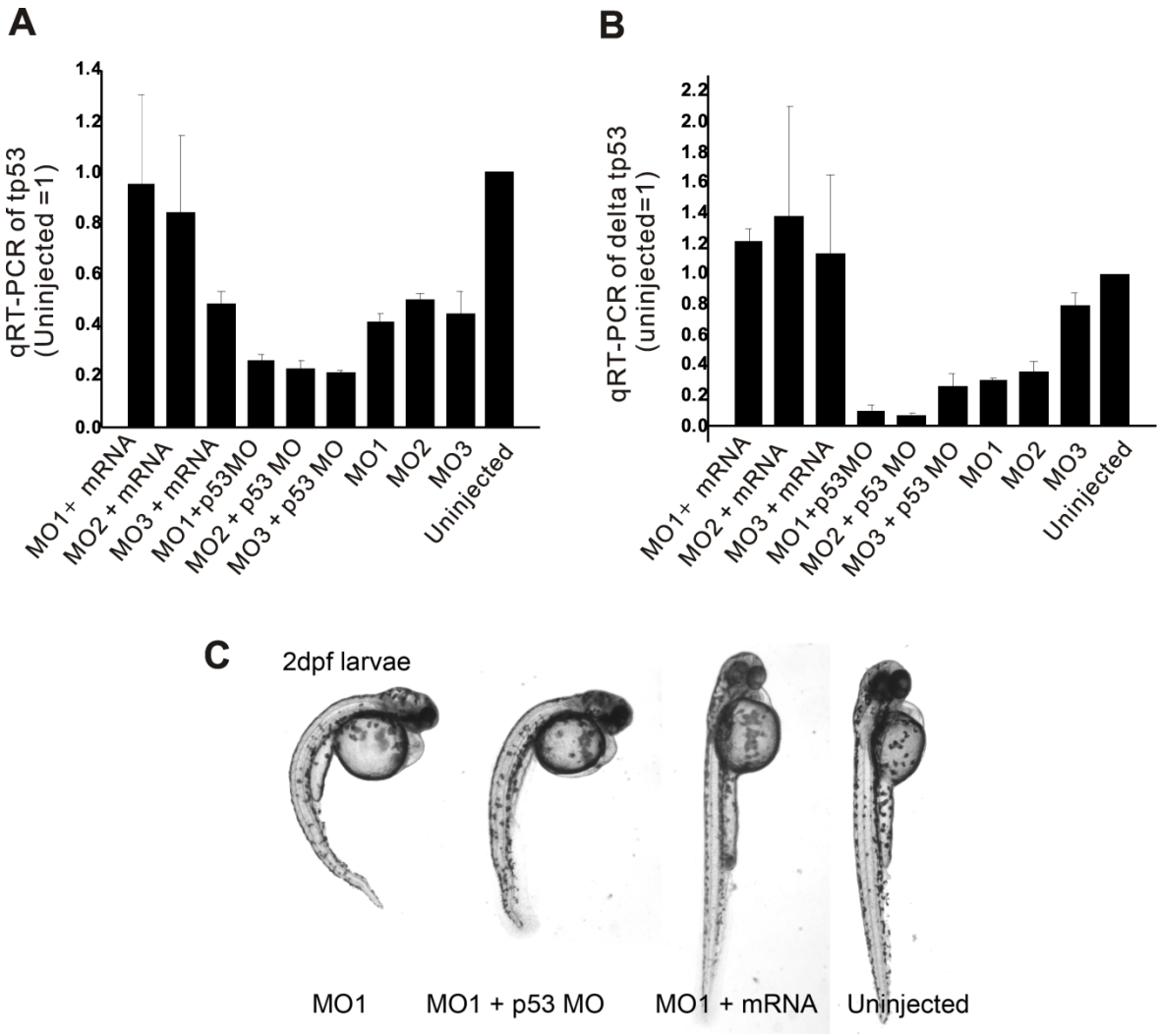
A
qRT-PCR of tp53 (Uninjected =1)
1.4
1.2
1.0
0.8
0.6
0.4
0.2
0.0
MO1+ mRNA
MO2 + mRNA
MO3 + mRNA
MO1+p53MO
MO2 + p53 MO
MO3 + p53 MO
MO1
MO2
MO3
Uninjected
B
qRT-PCR of delta tp53 (uninjected=1)
2.2
2.0
1.8
1.6
1.4
1.2
1.0
0.8
0.6
0.4
0.2
0.0
MO1+ mRNA
MO2 + mRNA
MO3 + mRNA
MO1+p53MO
MO2 + p53 MO
MO3 + p53 MO
MO1
MO2
MO3
Uninjected
C
2dpf larvae
MO1
MO1 + p53 MO
MO1 + mRNA
Uninjected